Satellite characterization using small aperture instruments at DRDC Ottawa

Robert (Lauchie) Scott, Brad Wallace
Defence Research and Development Canada

ABSTRACT

Small aperture telescopes used to obtain metric information can also provide a wealth of photometric detail on Deep Space satellites. Photometry of stabilized geostationary satellites as a function of phase angle can be used to classify objects based on bus type, and can be useful in identifying objects that have been cross-tagged in the satellite catalog. Photometric measurements sampled at rates faster than the spin rates of tumbling or spinning objects can provide additional detail about the objects. We present two cases of measurement on Canadian geostationary satellites. One case is to differentiate operational Canadian satellites from their cluster peers. The other is to identify the photometric signature of the decommissioned spacecraft.

1. INTRODUCTION

Small aperture optical telescopes have shown their utility in obtaining resident space object (RSO) metrics at a low cost [1]. Such systems use background stars and associated positions from high-quality star catalogs [2] to convert the pixel positions of the RSOs to a meaningful World Coordinate System. Star catalogs do not contain only star positions, however, but also include star brightness information – often in multiple colors. This raises the possibility that not only can RSO *positions* be measured, but their *brightness* can also be measured, opening the window for these inexpensive and productive systems to obtain and monitor signature information.

The Defence Research and Development Canada (DRDC) Space Surveillance Observatory (SSO) [1] is an example of a small aperture optical telescope designed to obtain metric data on Deep Space RSOs. The SSO has been operating for over a year and is able to obtain several hundred images each clear night. The automated data processing software has been designed to determine not simply the RSO positions, but the instrumental magnitude of the RSOs as well. The programming and computing cost of this capability is negligible, and as such the photometric data is available "for free" with each and every successful metric observation.

Photometric information can be useful for several purposes. On a simply pragmatic level, knowing the expected brightness of an object allows the system control software to more efficiently schedule observations such that intrinsically fainter objects are observed in more favorable conditions (i.e. phase angles), while intrinsically brighter objects can be observed in poorer – but nonetheless acceptable – conditions. In addition, knowing the expected relative brightness of two nearby RSOs can allow for more effective differentiation of cluster objects.

At a more strategic level, photometric signature data can yield basic Space Object Identification (SOI) information. The behavior of the satellite brightness as a function of phase angle, for example, is different from one satellite bus type to another, but is similar for multiple objects having the same bus [3]; as a result, examining this simple function can further aid in differentiation of cluster objects. Examining the photometry as a function of time for an uncontrolled or spinning spacecraft, on the other hand, can be used to help identify "lost" or misidentified objects. Color-based information is, of course, more effective yet, but since the DRDC SSO – like some other small telescopes designed for satellite metrics – does not routinely obtain color information, this will not be discussed further.

This paper will outline the operations and data reduction process for the DRDC SSO, with a specific emphasis on photometry-related issues. Having described how the photometric data are *obtained*, some examples will be given of how this data is actually *used*. First, an example will be shown of how the use of phase-angle light curve information was able to flag a probable mis-tag in the NORAD Satellite Catalog. A discussion of how this data can be used to schedule metric observations to help reduce mis-tags at the sensor level will be given. The second example will be of moderate cadence rate observations of a tumbling satellite, and how this data was able to serendipitously deduce some of the coarse features of the spacecraft.

2. PHOTOMETRIC CALIBRATION WITH THE SSO

The DRDC SSO is described in [1], and will not be discussed in depth here. The sensor system is based on Commercial Off The Shelf (COTS) components to leverage their testing heritage and low costs. The various components are presented in Table 1(taken from [1]).

Table 1: SSO sensor hardware components

Function	Component
Dome	10'6" Ashdome REB with electrically lowered screen
Dome Controller	ACE Smartdome
Optics	Celestron 14" optical telescope (f/11)
CCD Camera	Alta E-42 2048x2048 pixel camera, 13 micron pitch
Focuser	Optec TCF-S temperature compensating focuser
Filters	Optec IFW filter wheel with BVRI+clear filters (Bessel spec)
Sky Monitor	Boltwood Cloud Sensor
Environmental Enclosure	ITS Enclosures Icestation IS562626
Mount	Paramount ME Version II with MKS4000 controller
Telescope Control Software	TheSky6™ (using Orchestrate scripts)
CCD Control Software	CCDSoft™ ver 5

As briefly described in [1], one of the most important aspects of the SSO is its ability to automatically process the images in near-real time. The system uses the large number of background stars in the relatively large field of view of the sensor (22 arcminutes on a side) to provide an accurate conversion from CCD pixel-positions to the standard J2000 coordinate system. The processing software does this by comparing the positions of stars identified in the image data to the positions of stars listed in the USNO A2.0 star catalog [4].

One of the challenges inherent in doing photometry of RSOs is the fact that the RSOs are in constant motion with respect to both the background sky and with respect to the Earth's atmosphere. This is in contrast with stellar photometry, where the position of the target star stays in position with respect to nearby stars. The brightness of the target star can then be compared to the brightness of nearby stars (whether with or without precisely pre-determined brightness) to remove or minimize systematic effects due to sensor, atmospheric, or environmental changes.

Photometry of RSOs is not able to take advantage of these conditions (although for cluster differentiation, only relative magnitudes are required, not absolute), and ways have been found to roughly calibrate the photometric measurements for these objects. The first method – currently used in the automated processing software – is to use the background stars in a given frame to estimate the conversion from CCD pixel counts to stellar magnitudes, although this is not without issues. The SSO, when being used to obtain RSO metric information, collects image data in a filter-less mode while cataloged stellar brightness information is listed in one or more standard brightness bands, typically the Johnson UBVRI system [5]. This, coupled with the fact that the background stars will have varied colors, and the RSO itself has a color, will introduce a scatter in the conversion from counts to magnitudes. Further, this scatter will be different from image to image, and thus introduces uncertainty when comparing magnitudes from image to image.

Fortunately, it is possible to minimize this uncertainty by making some assumptions and doing some minimal post-processing of the photometry data. The key is the photometric zeropoint determined for each image. The zeropoint is the astronomical magnitude equivalent to a single CCD count, a value that depends on instrumental factors such as the telescope aperture, CCD gain, and quantum efficiency. This value changes only slowly over time, and so can be viewed as essentially constant for time periods of days to months. The key to comparing brightness information from image to image is thus to correct the derived zeropoint in each image such that they are constant over the course of a night or from night to night [6].

A caveat to this method is that it will yield brightness information that is consistent within the dataset, but which cannot be considered absolute in and of itself; thus, the brightness information is best considered as relative. A second caveat is that this method does not explicitly take into account any atmospheric reddening and is susceptible

to the resulting color variations. These effects are, for most purposes, not significant and do not stand in the way of producing useful results.

The second method for determining RSO brightness information is to characterize the sensor using stars of precisely determined brightness – "standard" stars, such as those listed by Landolt [5]. By observing groups of these standard stars at varying airmasses, and limiting comparison to stars of roughly solar colors, it is possible to determine a rough conversion between CCD counts and stellar magnitudes; this conversion can then be applied directly the RSO measurements to determine the associated magnitudes. This is the method that was used for the measurements discussed here. The standard error in the conversion is 0.3 magnitudes and the calibration curve used is shown in Figure 1.

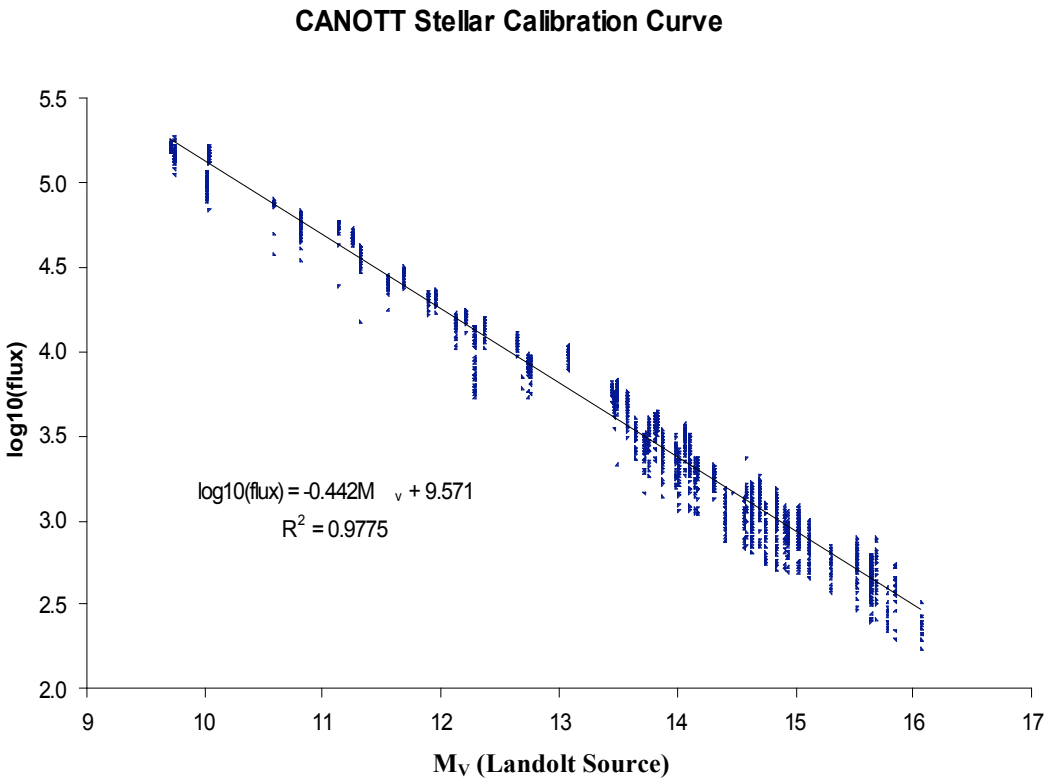

Figure 1: Calibration curve for the DRDC SSO

3. EXAMPLES

DRDC has been investigating the utility of photometric data obtainable using the SSO (and, potentially, other sensors designed for obtaining metric data such as the Canadian Concept Demonstrator system [7] and the upcoming NEOSSat spacecraft [8]). Two applications have been explored to date: phase angle based signatures - useful for scheduling, cluster discrimination, and satellite bus identification - and high time resolution "lightcurves" – to obtain spacecraft signatures for possible future identification, and which are potentially useful for understanding spacecraft morphology. Examples of this work shall be demonstrated here.

3.1 PHASE ANGLE BASED SIGNATURES

For the purposes of this investigation, observations were limited to Canadian deep-space satellites and satellites that are located in clusters containing Canadian satellites. Table 2 lists the observed satellites and their cluster peers.

Table 2: Canadian Geostationary satellites and cluster peers (with bus types[1])

Canadian Satellite(s) (bus type)	Longitude / Elevation	Cluster Peer(s) (bus type)
Nimiq 2 (LM A2100AX)	82.0 °W / 37.4°	DirectTV-3 (HS-601)
Nimiq 1 (LM A2100AX)	91.2 °W / 35.6°	DirectTV-1 (HS-601), Galaxy 11 (BSS-702C)
MSat M1 (HS-601)	106.4 °W / 29.3°	N/A
Anik F1 (BSS-702C)	107.3 °W / 29.3°	Anik F1-R (Eurostar 3000S)
Anik F1-R (Eurostar 3000S)	107.3 °W / 29.3°	Anik F1 (BSS-702C)
Anik F2 (BSS-702S)	111.0 °W / 27.4°	WildBlue-1 (LS-1300)
Anik F3 (Eurostar 3000S)	117.6 °W / 23.0°	Echostar-3 (occasional, not observed here))

Satellites in the geostationary ring are assigned station-keeping slots that span 0.1 degrees in longitude. Often several occupied slots fall within a range comparable to the field of view of the sensor: these are referred to as clusters. Usually the identification of a RSO in an image with a cataloged object is made simple because only a single cataloged object will be predicted to be in the field of view. In clusters, however, such assumptions are not applicable and other methods are needed to confidently identify the objects. The simplest method is to use position-based information, but the addition of additional prior knowledge, such as the brightness or colors of the various RSOs, can be helpful.

3.1.1 DATA COLLECTION

The data were collected using the SSO using Track Rate Mode (TRM), where the sensor is slewed at the rate, and in the direction of motion, of the spacecraft of interest. This increases the sensitivity of the system by concentrating the light of the RSOs on a handful of pixels instead of allowing the RSOs to streak and incur trailing losses. An example image of the image data obtained is shown in Figure 2.

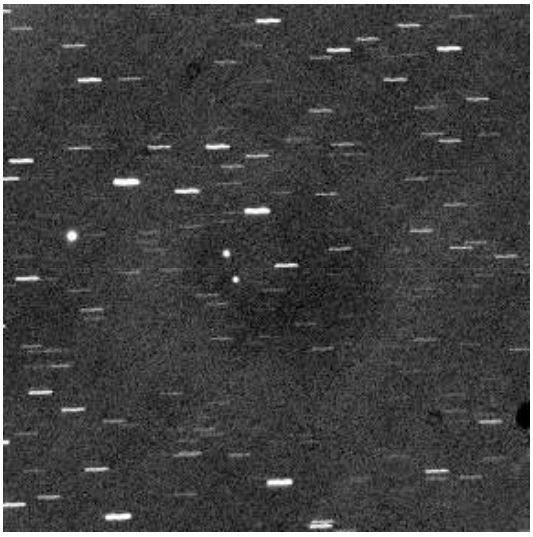

Figure 2: A typical TRM image obtained during the observing campaign. The RSOs are the point sources and the stars have been allowed to streak. From left to right, the three RSOs in this image are the Galaxy-11, DirectTV-1, and Nimiq-1 spacecraft.

[1] Boeing 702C (with solar panel concentrators), Boeing 702S (standard solar panels), Hughes Space 601 (HS-601), Lockheed Martin A2100AX (LM A2100AX), Loral Space 1300 (LS-1300) and Astrium Eurostar 3000S.

The data were collected during dedicated observing campaigns during three nights in early 2008. The campaigns started at nautical sunset and continued until nautical sunrise. The satellites were observed from the easternmost object to the westernmost object using TLEs accurate for that date. Two images are collected for each object at a given time in order to minimize issues resulting from confusion with star streaks. After reaching the westernmost object the telescope slewed back to the easternmost object and repeated the cycle until sunrise. Each east-to-west observing cycle takes roughly 5 minutes.

Table 3: Selected observing parameters

Item	Value
Campaign dates	24, 25 February, 17 March, 2008
Observing Mode	Track Rate
Exposure times	4s
Pixel size	2.1 arcseconds
Field of view	0.4 degrees x 0.4 degrees
Sensitivity	14.5 magnitude

In keeping with the standard operation of the SSO, after the data are observed the image is pushed to a data reduction server that automatically processes the data. Tying the counts to Landolt standard stars, as described earlier converted the CCD counts to magnitudes. The data were then normalized to a common slant range of 36,000 km for comparison.

3.1.2 BULK SATELLITE PHASE CURVES

The collected data for all satellites over the three observing sessions is shown in Figure 3. The data are color coded according to satellite bus type and are plotted as instrumental magnitudes versus phase angles. The position-based correlation uses the TLEs of date as supplied by NORAD.

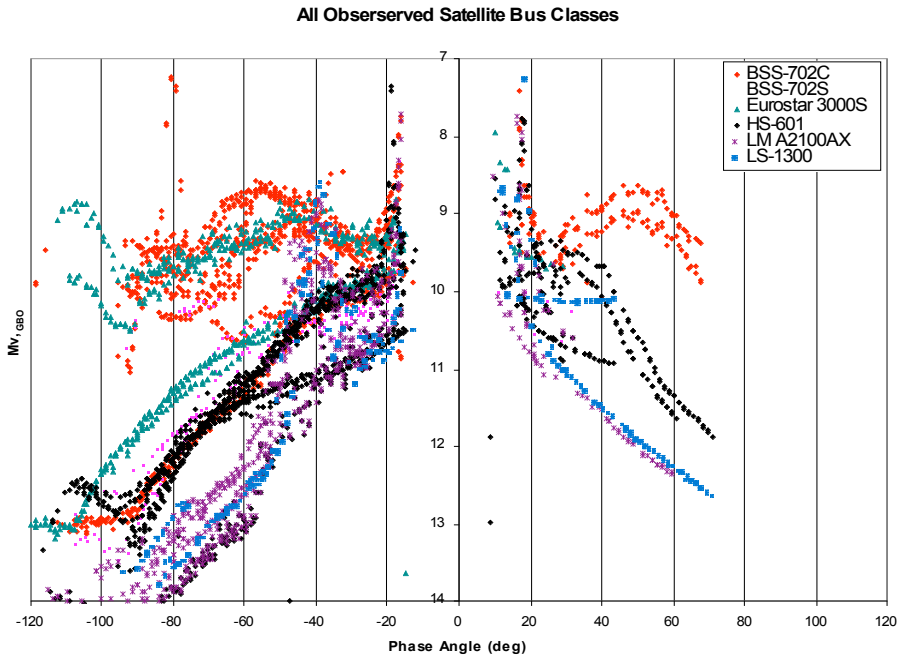

Figure 3: Instrumental phase angles versus phases angle for all observing sessions. The data are color coded according to bus type. When the phase angles are opening the angle is said to be positive (+) while when it is closing the angles are negative (-)

As expected, satellite brightness generally increases as the phase angle (defined as the sun-RSO-sensor angle) approaches zero. The dramatic increase in brightness inside of 20 degrees phase angle is due to specular reflection off of solar panels. The absence of data between -15 and +10 degrees phase angle is due to the satellites entering Earth's shadow. The asymmetry in phase angle coverage from eastern (negative) to western (positive) phase angles is due to the onset of sunrise and the relative observing geometry.

A cursory examination of Figure 3 reveals that that there are recurring trends in the curves for each type of satellite bus, supporting the expectation that such light curves can be used to classify the bus types of unknown spacecraft. (A deeper examination suggests that there are two deviations from this general trend – these will be discussed below). A further examination shows that there are subtle shifts in many of brightness curves, attributable to night-to-night variations in either satellite brightness (due to changing solar declination) or potentially sensor calibration.

3.1.3 INTRA-CLUSTER COMPARISONS

Figure 4 displays the magnitude-phase light curves organized by Canadian geostationary satellites and their cluster peers. A number of individual features can be noted – the glints seen in Nimiq-1 and Nimiq-2 near -40 degrees phase angle, the near linear curve for Galaxy-11, and the depression in brightness near -90 degrees for MSat-M1, for example – but some bulk conclusions can also be drawn. For example, in each cluster the spacecraft have very different light curves, suggesting that a single relatively dedicated observing campaign could help separate mistags.

For routine metric observations a less observation-intensive solution can also be suggested: simply observe the objects at phase angles of roughly -60 degrees. At this phase angle the spacecraft are still relatively bright – certainly within the sensitivity range of the DRDC SSO for example – but the difference in satellite brightness for the cluster peers are typically on the order of a full magnitude – sufficient to help correctly tag the sources without requiring additional observing.

A specific note, however, concerns the Anik-F1/Anik-F1R cluster. While the two spacecraft have significantly different magnitude-phase angle behavior, a closer examination suggests that the two spacecraft have been – in fact – mistagged in the NORAD Satellite Catalog of date. This possibility arises when comparing the light curve of Anik-F1 (having a BSS-702C bus) with Galaxy-11 (which also has a BSS-702C bus). The two light curves are distinctly different, but the nearly linear magnitude/phase-angle light curve of Galaxy-11 is very similar to the observed light curve of Anik-F1R (which has a Eurostar 3000S bus). Comparing the observed light curve of Anik-F1R with that of the other observed Eurostar 3000S satellite, Anik F3, we again see distinct differences.

Based on these observations the suspicion of a mistag becomes strong. Given that Anik F3 does not have a cluster peer with which to be confused, the light curve of Anik F3 can be reasonably associated with the Eurostar 3000S bus. This light curve is very similar to the observed light curve associated with Anik F1 – right down to the linear "foot" at -100 degree phase angle - suggesting that the object tagged as Anik F1 is instead Anik F1R, and the object tagged Anik F1-R is instead Anik F1. Further, the mistag appeared to be within the NORAD TLE data itself, since the relative observed and predicted positions of the spacecraft resulted in the mistagging. The possible mistag was reported to SSN analysts.

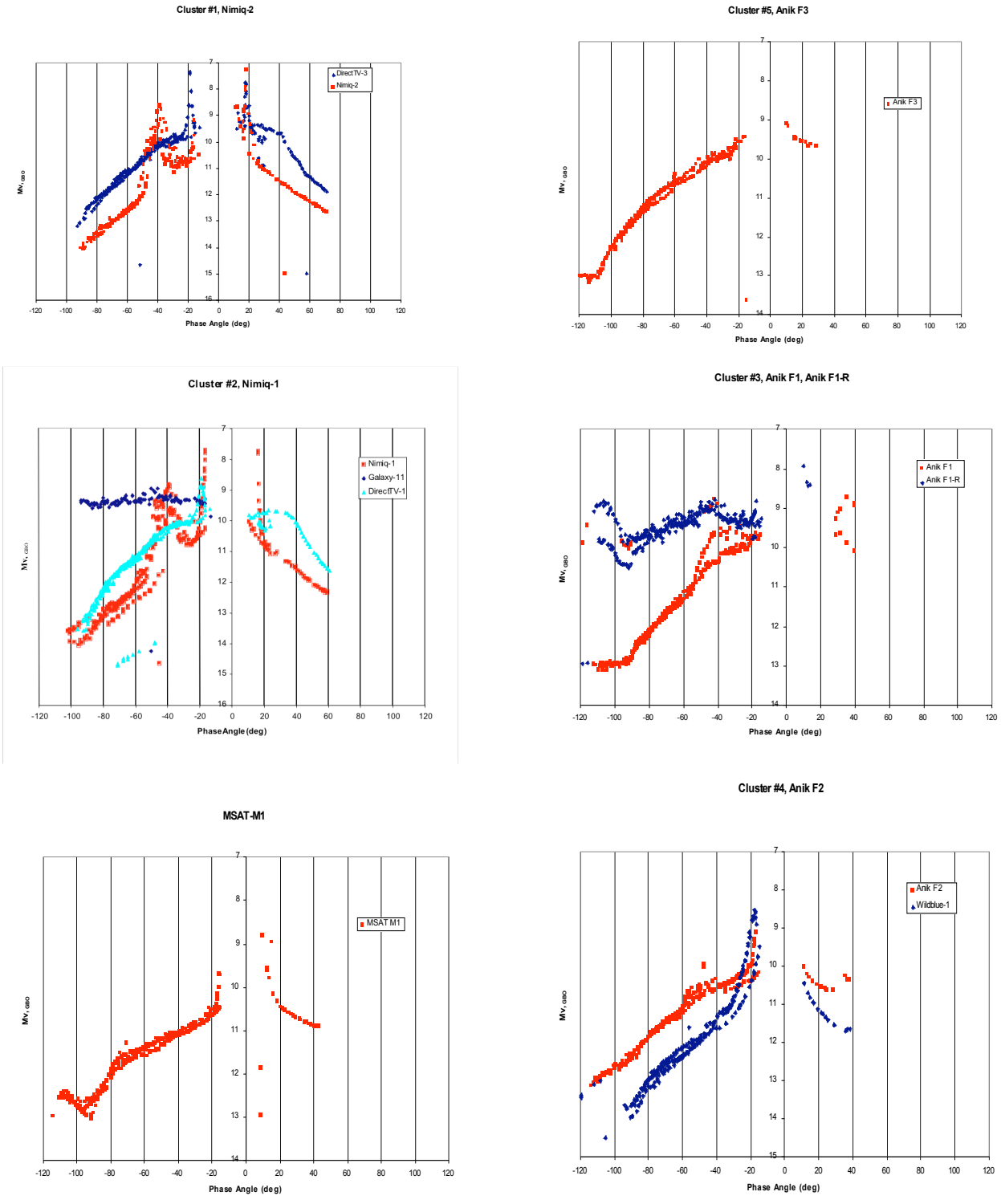

Figure 4: Magnitude-phase light curves of Canadian Geostationary satellites and cluster peers.

3.2 "HIGH" RATE PHOTOMETRY

3.2.1 DATA COLLECTION AND REDUCTION

Light curve data were obtained for two tumbling spacecraft – Telstar 401 and Anik D1. The SSO was not designed for true high speed observing, and so the observation cadence is limited by the CCD readout rate. The images were exposed for 0.5s and are separated by 4.2s. The data were taken on the nights of December 8/9, 2007 (Telstar 401) and December 14/15 (Anik D1). As previously, the data were obtained in TRM to increase sensitivity and reduce stepped slewing action of the mount. The brightness of the spacecraft was not tied to the Landolt standard stars, but the flux in the images are instead measured relative to each other. The data are presented in arbitrary units. The data were collected for about 20 minutes for each spacecraft.

After the observations were processed to determine the RSO brightness, the periodicity of the time series was determined using a Fourier Transform.

3.2.2 TELSTAR 401

The time series for the Telstar 401 observation is shown in Figure 5. The data clearly show the periodicity of 165.7s seconds. The obvious features include a strong peak of varying intensity along with three smaller sub-peaks.

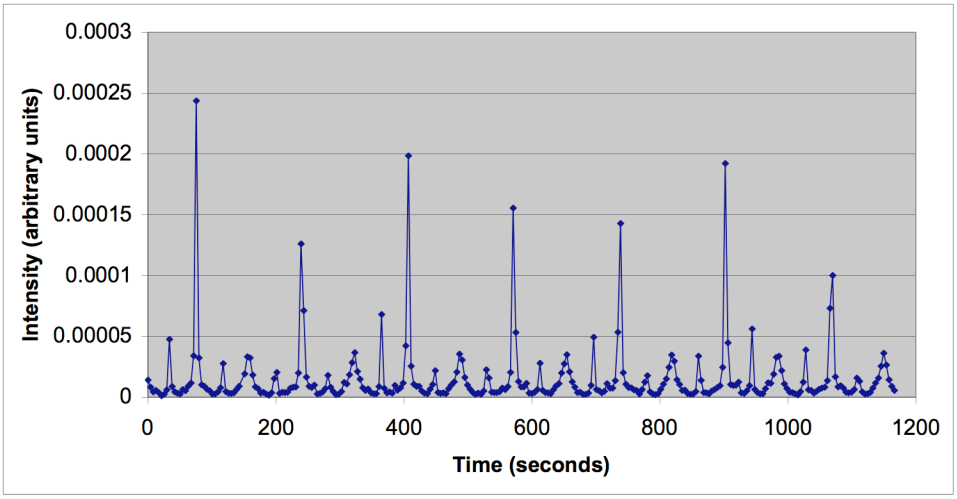

Figure 5: Telstar 401 time series data

In order to better understand the time series, a play was taken from the playbook used by pulsar astronomers [9] and the observed data were "folded" to improve the sampling in phase. Essentially, the data from the second and subsequent cycles were shifted backward in time by (cycle number times the period) seconds so that a single, well sampled, cycle is created. This folded light curve is shown in Figure 6; two cycles are shown for clarity, but the second period is simply the first period replicated.

The features of the light curve now stand out more clearly. The varying peaks seen in Figure 5 are revealed to simply be the peak sampled at different points in phase and thus sampling different brightness; the folding process brings these into their correct orientation. The three sub-peaks are also more clearly seen here and reveal an interesting feature – the middle sub-peak is considerably broader, and somewhat fainter, that the two other sub-peaks.

Telstar 401 has a "box with wings" configuration, and the current working explanation is that the main peak and two other sub-peaks – all three of which are very narrow- are specular reflections off the front of the solar panels (main peak) and the sides of the bus (sub-peaks). The broad sub-peak, however, is thought to originate from diffuse reflection off the back of the solar panels. Engineers who have worked on Telesat spacecraft [10] confirm the

plausibility of this conjecture by noting that the backs of solar panels were routinely painted with a diffuse black paint to help remove heat from the spacecraft.

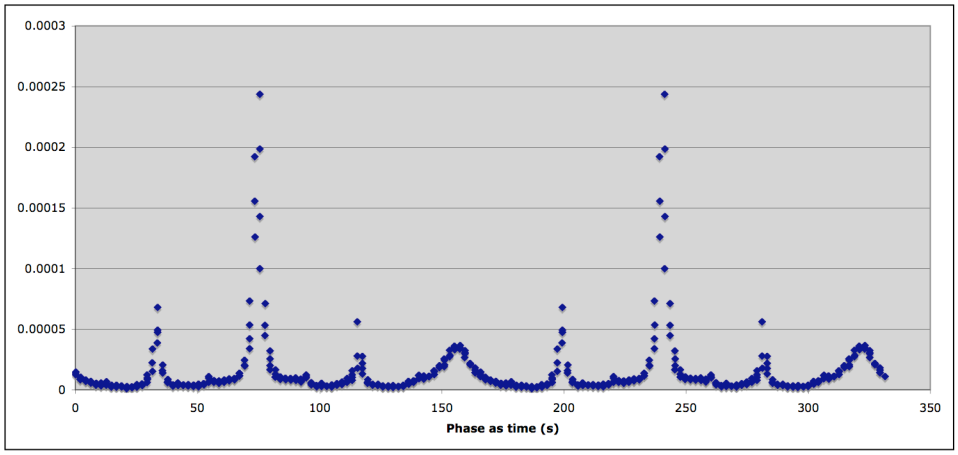

Figure 6: "Folded" Telstar 401 lightcurve; two cycles are displayed, but the second cycle is a simple replication of the first.

3.2.3 ANIK D1

The analysis of Anik D1 is not so clear-cut as for Telstar 401. No obvious patterns emerge from the raw light curve (Figure 7).

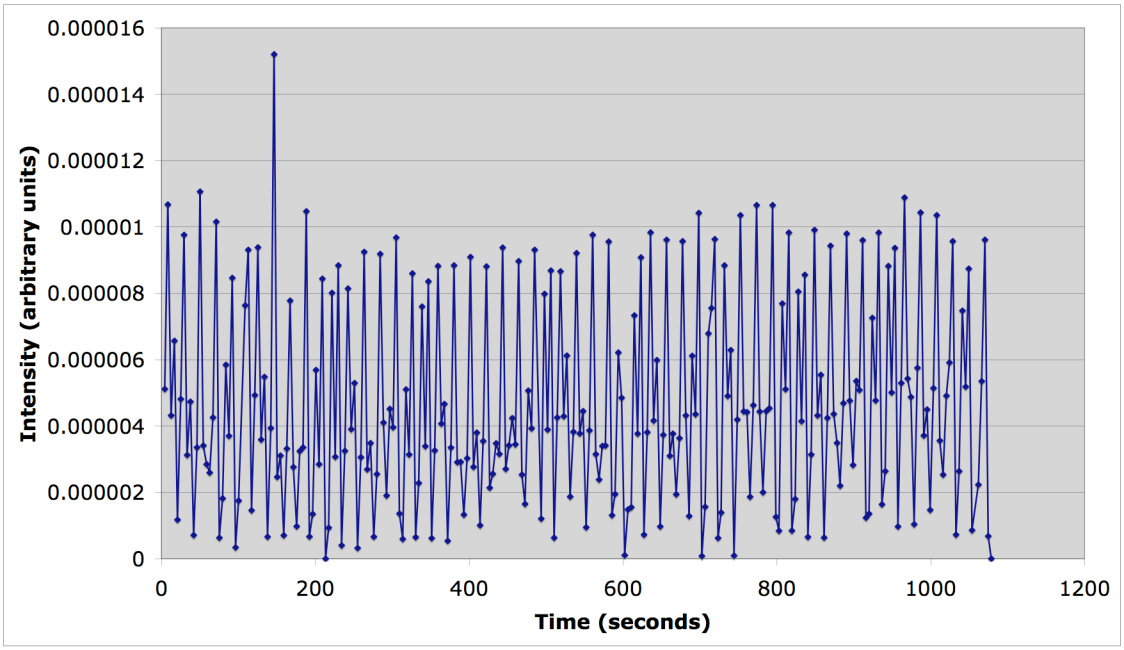

Figure 7: Anik D1 light curve.

The FFT of the data has a strong peak at roughly 3.08 cycles/min, and another at 5.65 cycles/min. Folding the light curve at the derived period does not significantly improve matters (Figure 8).

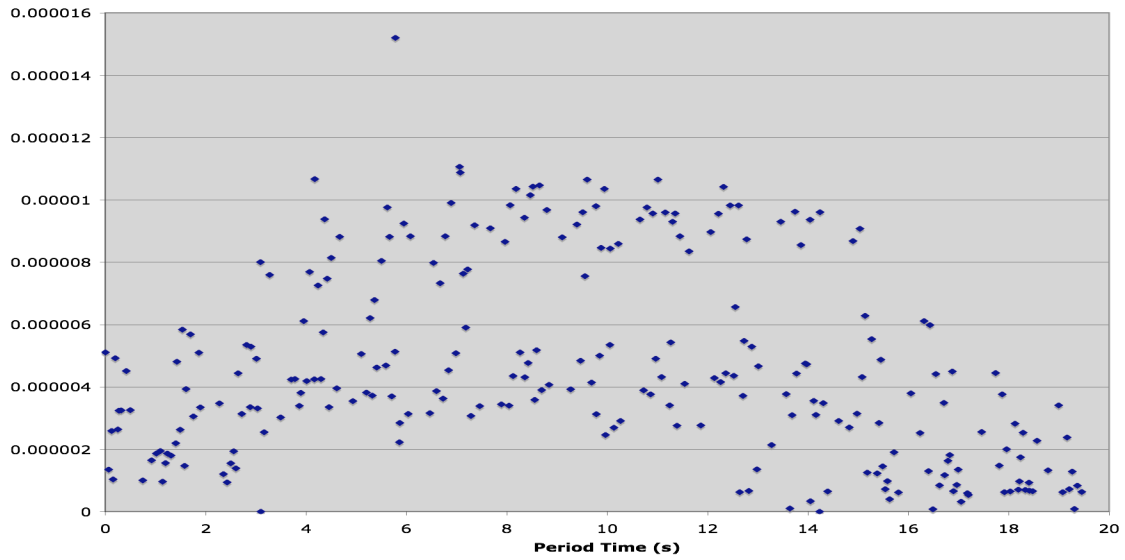

Figure 8: Folded light curve for Anik D1. A single cycle, folded at a period of 3.08 seconds, is shown

While there is a hint that useful signature information may exist within the data, there is significant scatter that suggests there may be multiple trends being manifested simultaneously. More work remains to be done to understand the light curve behavior of this spacecraft.

4. DISCUSSION AND CONCLUSION

This paper demonstrates some of the utility and limitations of photometric data obtained using a passive optical sensor designed for satellite metrics. The issue of calibrating the photometry was briefly discussed, but it is clear that the methods used do not yield an absolute scale: the values shown in this paper should be treated as rough, with a maximum precision and accuracy of 0.3 magnitudes.

Two examples of photometric data were shown. The first – characterization of satellites based upon the variation of their brightness with respect to phase angle – demonstrates not only that spacecraft buses can be characterized in this way, but also that spacecraft in clusters can be usefully discriminated based upon this information. Specifically, while full "lightcurves" can be created, discrimination can take place as long as the observations took place at around -60 degrees phase angle, where significant differences in expected brightness can be expected.

It is worth noting a few caveats to these conclusions. First, the data presented here were obtained over a short time during one season. Specific features – the shadow region, specular reflections – would not be seen in observations taken at different seasons. As such, regular characterization of the spacecraft over the period of a year (say, once a month) should be conducted before using this data in practice.

The second example – higher rate photometry – demonstrated the ability to derive a clear signature of the spacecraft that is consistent with plausible assumptions about the spacecraft shape and construction. The limit to this sort of investigation is that the data must be sampled at a rate that is a small fraction of a tumble period, and the integration period for a single measurement should likewise be a small fraction of a period.

With these caveats in mind, however, it is clear that useful photometric information can be gleaned from a small optical sensor designed for use in obtaining metric information.

5. References

1. Wallace, B., Scott, R.L., Spaans, A., "The DRDC Space Surveillance Observatory", AMOS Technical Conference 2007, Maui HI

2. Zacharias, N., Urban, S.E., Zacharias, M.I., Wycoff, G.L., Hall, D.M., Monet, D.G., Rafferty, T.J., *The second US Naval Observatory CCD Astrograph Catalog (UCAC2)* Astronomical Journal, 2004. **127**
3. Payne, T., "SSA Analysis of GEOS Photometric Signature Classifications and Solar Panel Offsets", AMOS Technical Conference 2006, Maui HI.
4. Monet, D., Bird, A., Canzian, B., Dahn, C., Guetter, H., Harris, H., Henden, A., Levine, S., Luginbuhl, C., Monet, A.K.B., Rhodes, A., Riepe, B., Sell, S., Stone, R., Vrba, F., Walker, R., USNO-A2.0 A Catalog of Astrometric Standards, available on the WWW at http://tdc-www.harvard.edu/software/catalogs/ua2.html, accessed 11 August 2008.
5. Landolt, A., "UBVRI Photometric Standard Stars in the Magnitude range of 11.5<V<16.0 Around the Celestial Equator" Astronomical J. vol. 104, no. 1, July 1992.
6. Sydney, P., Africano, P., Kelecy, T., High Precision Satellite Astrometry and Photometry, 2004 AMOS Technical Conference, Maui, HI, Sept 2004
7. Wallace, B. "A Canadian array of ground-based optical sensors for deep space monitoring," 2003 AMOS Technical Conference, Maui HI, Sep 2003
8. Wallace, B, et al, "The Near-Earth Orbit Surveillance Satellite (NEOSSat)", International Astronautical Congress, October 2004.
9. Lorimer, D.R., Kramer, M., Handbook of Pulsar Astronomy, Cambridge University Press, 2005
10. Burlton, B., private communication